

Aleksandra Piórkowska-Kurpas

Matter To The Deepest Recent Developments In Physics Of Fundamental Interactions XLVI International Conference of Theoretical Physics

15-19 września 2025



Centre for Creativity and Coworking



University of Silesia, August Chełkowski Institute of Physics

Division for Physics of Fundamental Interactions Polish Physical Society





Deflection of the light path near massive body can be calculated within

Newtonian theory of gravity:

test particle with velocity v moving past an object of mass M is deflected by

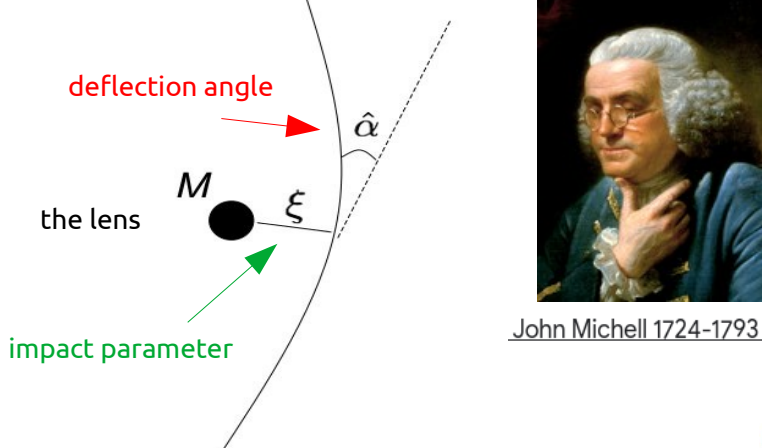
$$\hat{\alpha} = 2GM/(v^2\xi)$$

if light treated as particles

$$\hat{\alpha_{\mathrm{N}}} = 2GM/(c^2\xi)$$

[Mitchell 1784; Soldner 1804]

after S. Suyu; lectures XXIV Canary Islands Winter School of Astrophysics 2012





Johann Georg von Soldner

But the deflection angle drived from GR is as twice as it!

 $\hat{\alpha_{\rm E}} = 4GM/(c^2\xi) = 2\hat{\alpha_{\rm N}}$

[A. Einstein (1915); proved by A. Eddington in 1919]

problem of photon orbits in Schwarzschild geometry



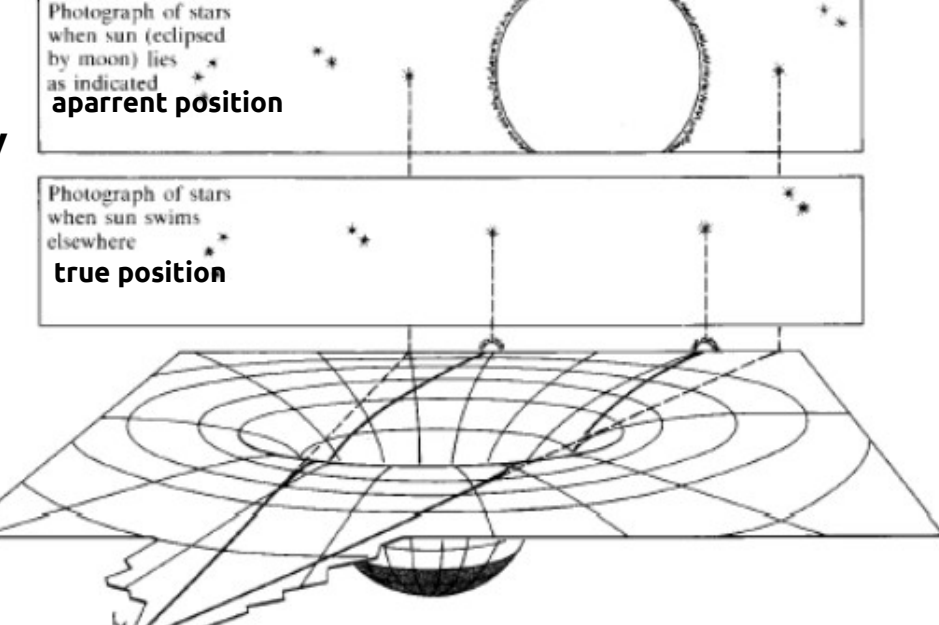


Albert Einstein

Sir Arthur Eddington

National Maritime Museum, Greenwich

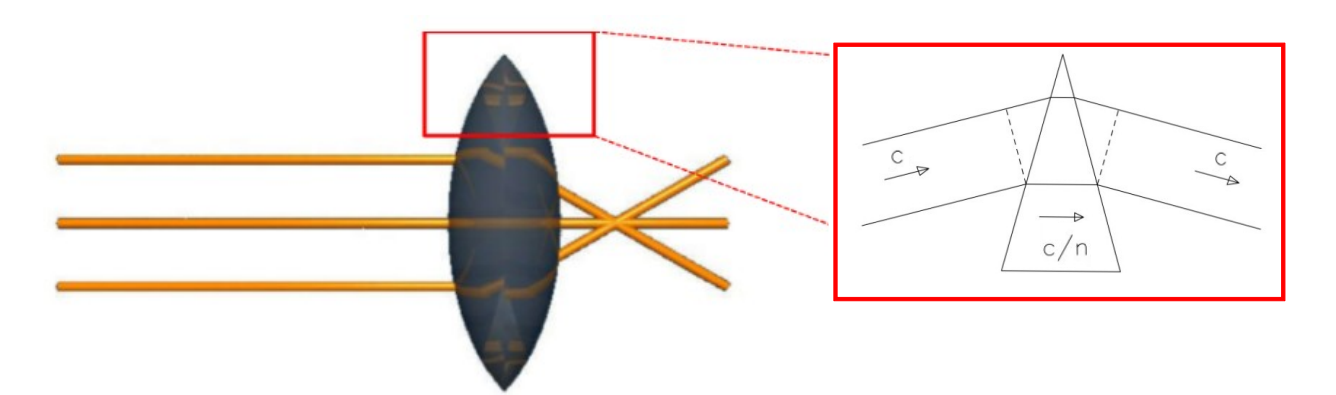
Solar eclipse, 29 May 1919 [Sobral/Principle Island]



1.75 arc seconds for light nearly grazing the outside of the sun

The effect of spacetime curvature on the light paths can be expressed in terms of an effective index of refraction n:

[Schneider et al.1992]



in classical optics lens bends light rays due to the difference in refractive index between lens material and surrounding medium

but in vacuum n=1!

Deflection is the integral along the light path of the gradient of n perpendicular to the light path

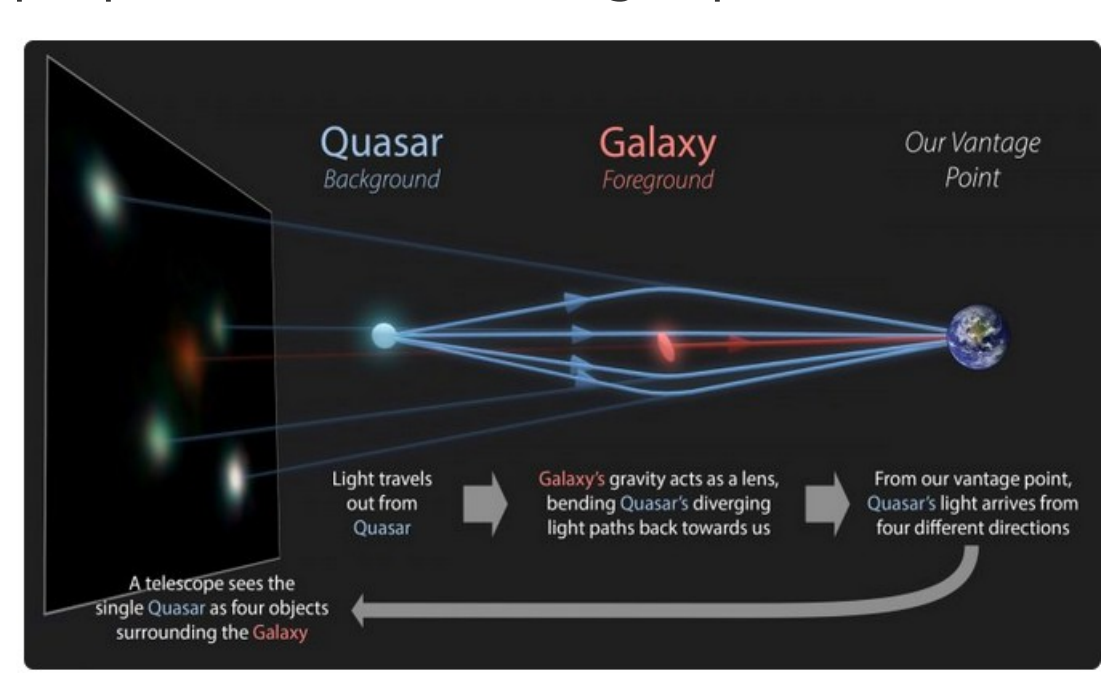
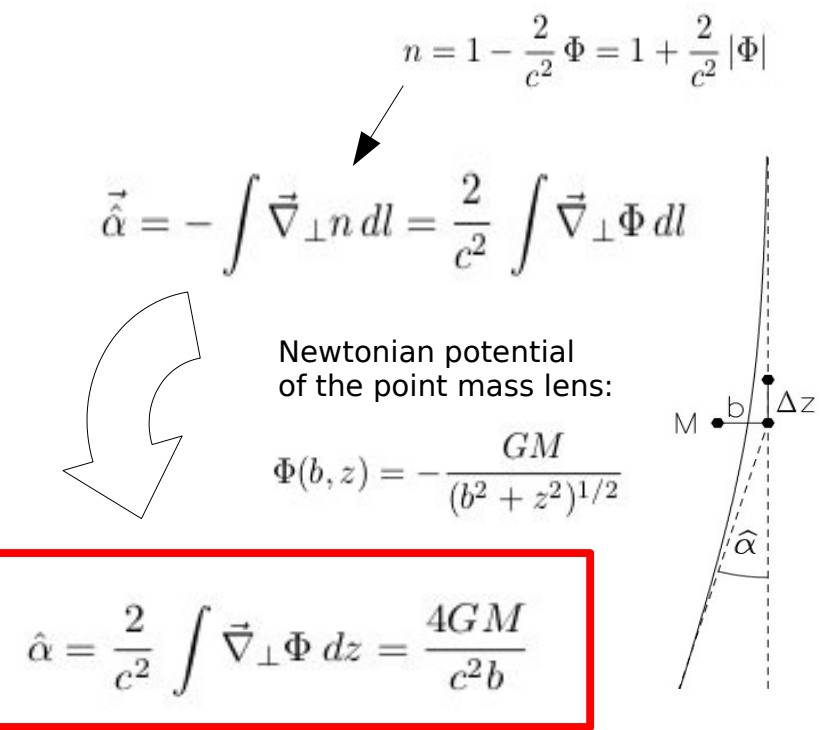
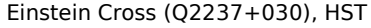


Image via R. Hurt (IPAC/ Caltech)/ The GraL Collaboration/ ESA.



Different regimes of gravitational lensing:

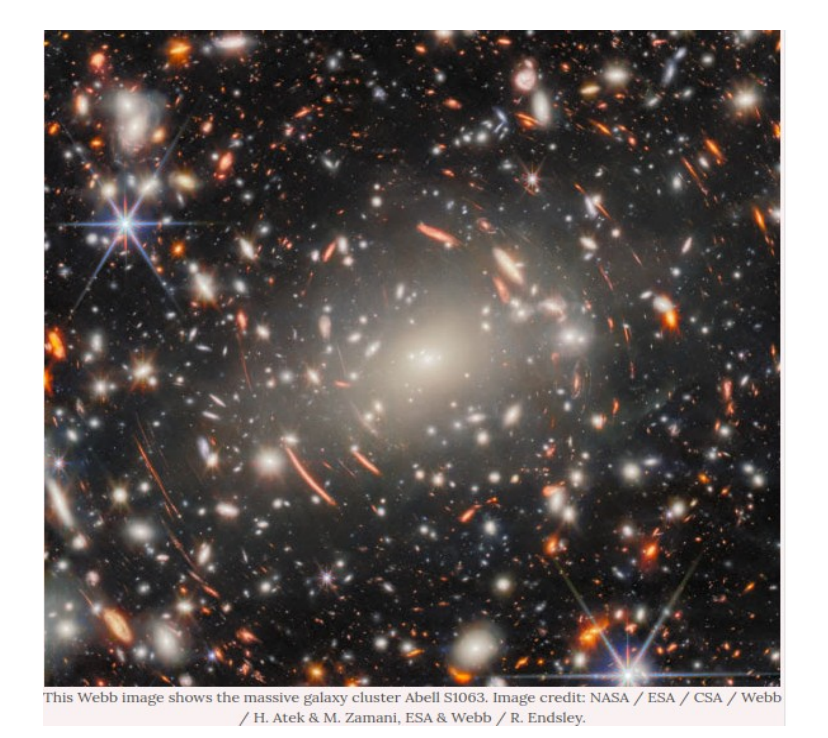






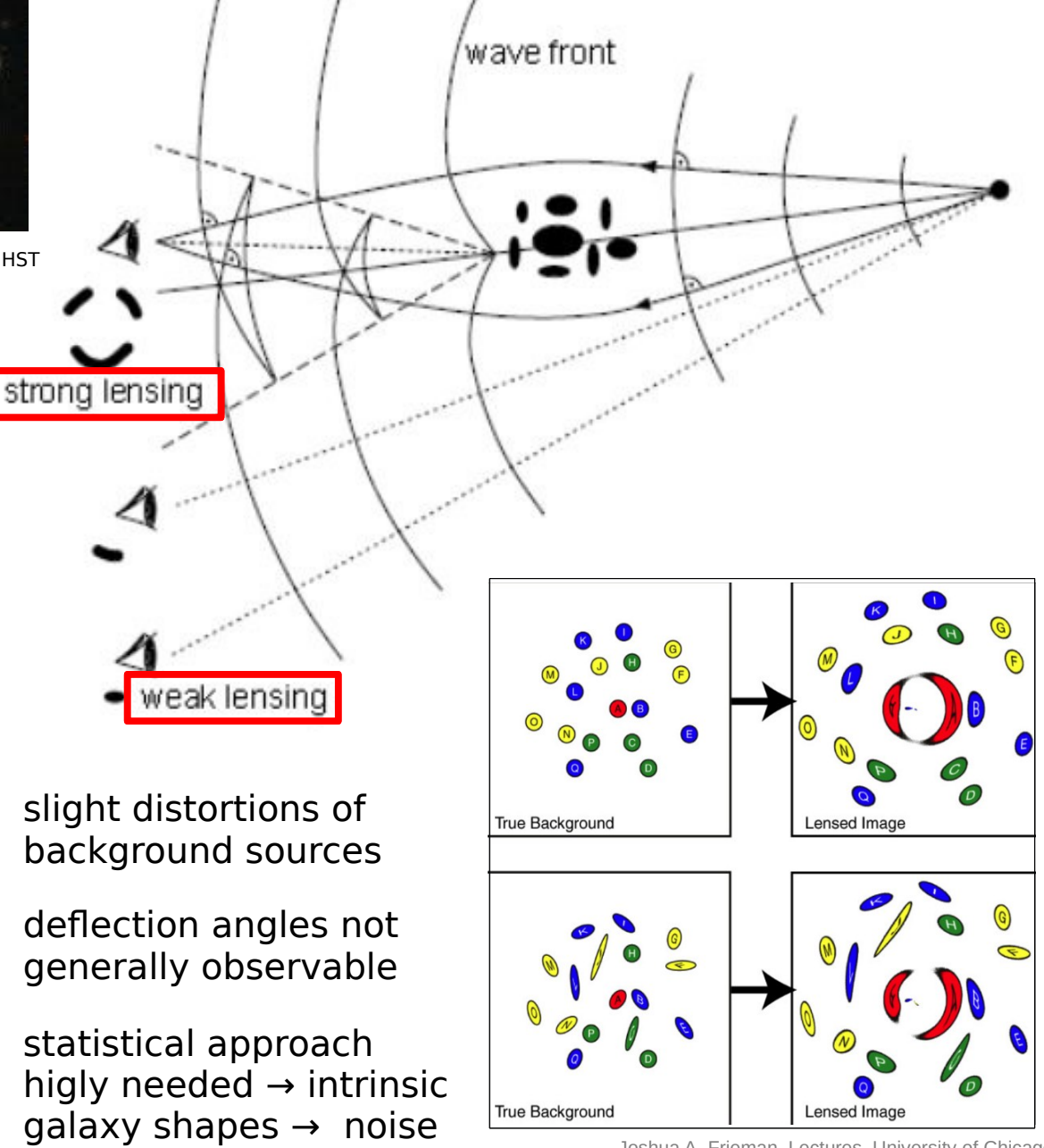
Cosmic Horseshue (SDSS J1148+1930), HST

- multiple images
- time delays between images
- images distorted into rings/arcs



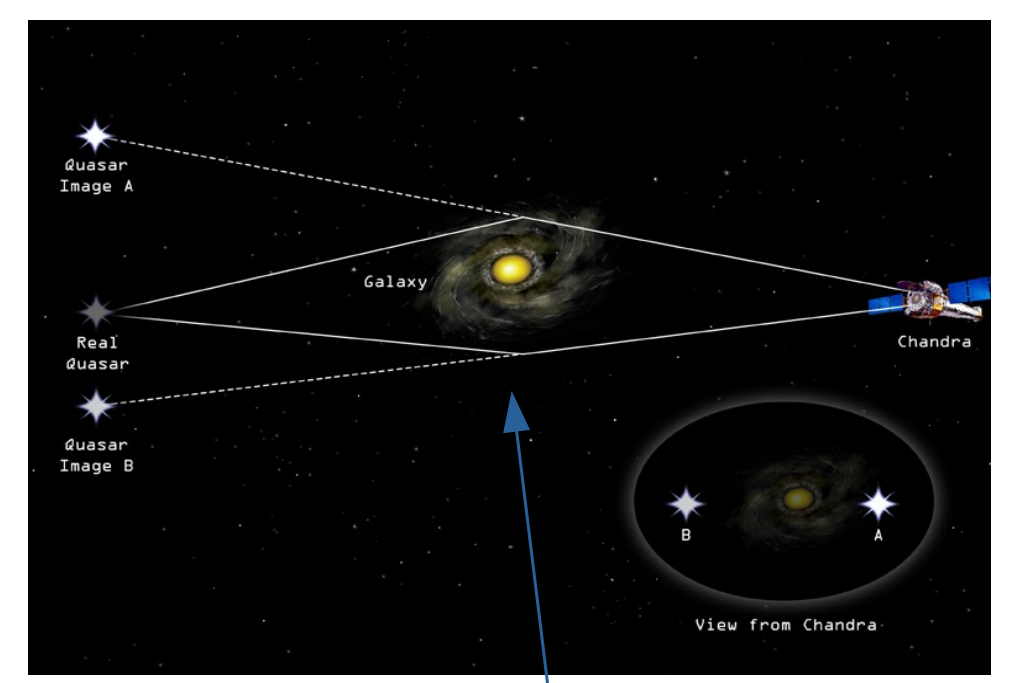
slight distortions of background sources

- deflection angles not generally observable
- statistical approach higly needed → intrinsic galaxy shapes → noise



Joshua A. Frieman, Lectures, University of Chicago

Strong gravitational lensing:



https://chandra.harvard.edu/

effective lesing (Fermat) potential

 $\phi(\boldsymbol{\theta}) = \frac{D_{ls}}{D_{l}D_{s}} \frac{2}{c^{2}} \int \Phi(D_{l}\boldsymbol{\theta}, z) dz$

Travel time of light rays from images \rightarrow time delay:

$$\Delta t = rac{1+z_{
m l}}{c} rac{D_{
m ol} D_{
m os}}{D_{
m ls}} \left[rac{(m{ heta}-m{eta})^2}{2} - \phi(m{ heta})
ight]$$
Massimo Meneghetti, Introduction to Gravitational Lensing; Lecture scripts

Newtonian

plane

potential at lens

 $t_{
m grav}$

Schneider, Ehlers, Falco.

 $t_{\rm geom}$ 'Gravitational Lenses' Schneider, Kochanek, Wambsganss, 'Gravitational Lensing: Strong, Weak and Micro'

in the light ray formalism:

(thin screen approximation)

$$oldsymbol{\eta} = rac{D_{
m s}}{D_{
m d}} oldsymbol{\xi} - D_{
m ds} oldsymbol{\hat{lpha}}(oldsymbol{\xi})$$

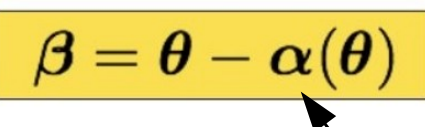
In terms of angular coord.:

$$\boldsymbol{\eta} = D_{\mathrm{s}}\boldsymbol{\beta}$$

$$\boldsymbol{\xi} = D_{\mathrm{d}} \boldsymbol{\theta}$$

 $\alpha = \nabla_{\theta} \phi$

lens equation



reduced deflection angle

$$rac{D_{
m ds}}{D_{
m s}} m{\hat{lpha}}(D_{
m d}m{ heta})$$

Lens plane

Observer

Schneider, 2006

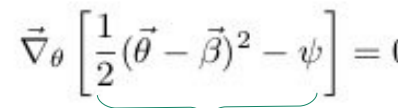
Bartelmann& Schneider, 2001

S. Suyu; lectures XXIV Canary Islands

Winter School of Astrophysics 2012

$$\vec{\nabla}_{\theta} \left[\frac{1}{2} (\vec{\theta} - \vec{\beta})^2 - \psi \right] = 0$$

Fermat potential



Fermat Principle





Pierre de Fermat

Images are located at points where the total time delay function is stationary



Magnification and distortion:

main features of gravitational lensing!

Liouville's Theorem

Lensing conserves surface brightness Flux F = surface brightness x solid angle Magnification = $F_{observed}$ / $F_{intrinsic}$ = $d\Omega_{observed}$ / $d\Omega_{intrinsic}$



Joseph Liouville

after S. Suyu; lectures XXIV Canary Islands Winter School of Astrophysics 2012

Jacobian matrix for gravitational lensing:

$$\mathcal{A}(\boldsymbol{\theta}) = \frac{\partial \boldsymbol{\beta}}{\partial \boldsymbol{\theta}} = \left(\delta_{ij} - \frac{\partial^2 \phi(\boldsymbol{\theta})}{\partial \theta_i \partial \theta_j}\right) = \begin{bmatrix} 1 - \kappa - \gamma_1 & -\gamma_2 \\ -\gamma_2 & 1 - \kappa + \gamma_1 \end{bmatrix}$$

shear

$$egin{align} \gamma &\equiv \gamma_1 + \mathrm{i} \gamma_2 = |\gamma| \mathrm{e}^{2\mathrm{i} arphi} \ \gamma_1 &\equiv rac{\partial \phi}{2\partial heta_1 \partial heta_1} - rac{\partial \phi}{2\partial heta_2 \partial heta_2} \ \gamma_2 &\equiv rac{\partial \phi}{\partial heta_1 \partial heta_2} \ \end{array}$$

stretches source image tangentially around the lens

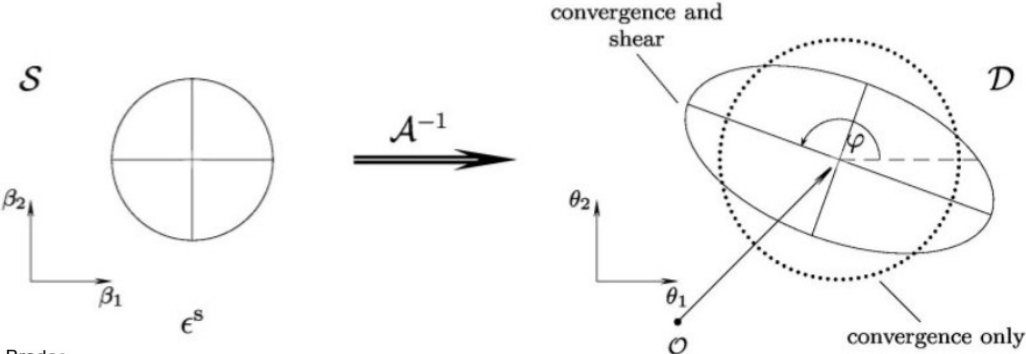
convergence

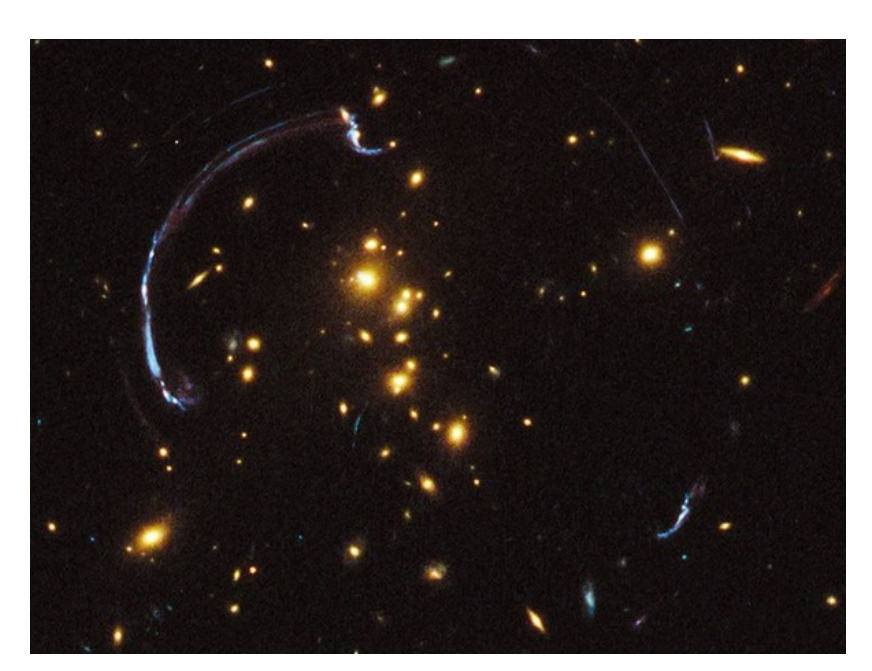
$$\kappa = rac{\partial \phi}{2\partial heta_1 \partial heta_1} + rac{\partial \phi}{2\partial heta_2 \partial heta_2}$$

magnifies source image by increasing its size

Magnification in terms of κ and γ is:

$$\mu = \frac{1}{\det \mathcal{A}} = \frac{1}{(1 - \kappa)^2 - |\gamma|^2}$$

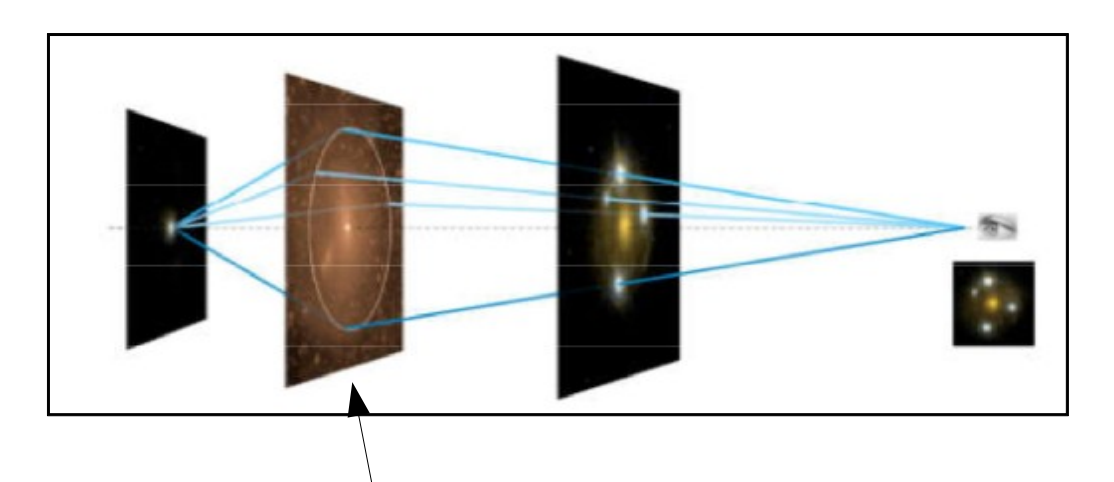




Galaxy Cluster RCS2 032727-132623 (HST image/NASA)

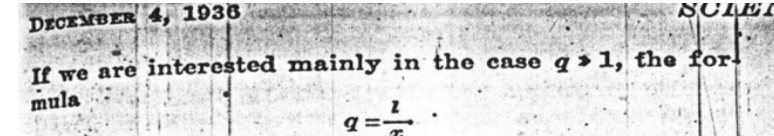
magnification

$$\mu(\boldsymbol{\theta}) = \frac{1}{\det A(\boldsymbol{\theta})}$$



Einstein ring -

introduces angular scale characteristic of a given lensing c



is a sufficient approximation, since $\frac{x^2}{l^2}$ may be neglected. Even in the most favorable cases the length l is only a few light-seconds, and x must be small compared with this, if an appreciable increase of the apparent brightness of A is to be produced by the lens-like action of B.

Therefore, there is no great chance of observing this phenomenon, even if dazzling by the light of the much nearer star B is disregarded. This apparent amplification of q by the lens-like action of the star B is a most curious effect, not so much for its becoming infinite, with x vanishing, but since with increasing distance D of the observer not only does it not decrease, but even increases proportionally to \sqrt{D} .

ALBERT EINSTEIN

INSTITUTE FOR ADVANCED STUDY, PRINCETON, N. J.



Einstein radius

$$\theta_E = \sqrt{\frac{4GM}{c^2} \frac{D_{LS}}{D_L D_S}}$$



for the lens of 1 M_☉ and for typical galactic distances of 10 kpc

$$\theta_E$$
 ~ 0".001

unobservable!



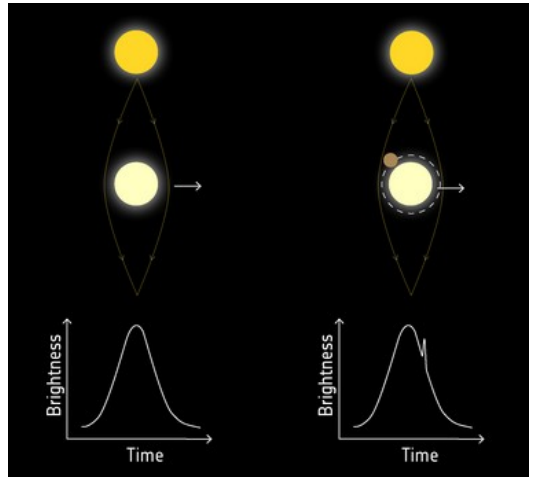
strong lensing of stars by a star:

- small value of deflection angle
- $_{ imes}$ $\,$ unlikely alignment requirement for lensing

"there is no great chance of observing this phenomenon"

[Einstein, 1936]

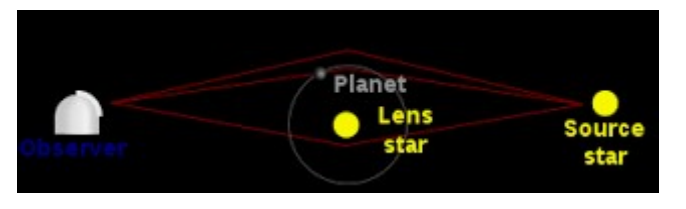






MICROLENSING!

<u>prof. Bohdan Paczyński</u>



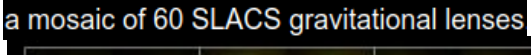
F.Zwicky (1937): multiple images can be detected if one consider deflector as more massive than stars, e.g. galaxies



The first observation:

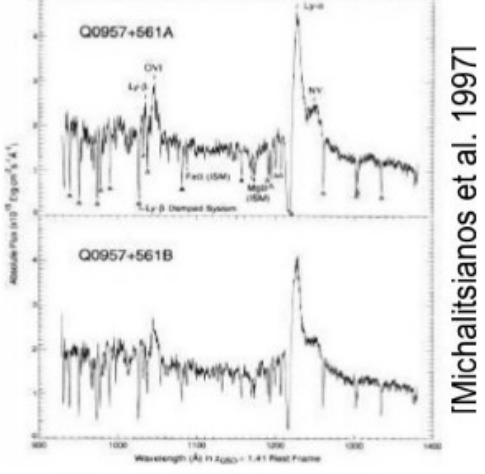
double quasar QSO-0957+561A,B
Walsh, Carswell & Weynmann 1979

 1978-1992 – only 11 strong lensing systems was discovered









identical spectra!

Era of massive galaxy surveys:

now we know hundreds of strong lensing systems!

SLACS, BELLS, CFHT – SL2S, CLASS, SQLS, HAGGLeS, AEGIS, COSMOS, CASSOWARY



spectroscopic searches concentrated on sources!

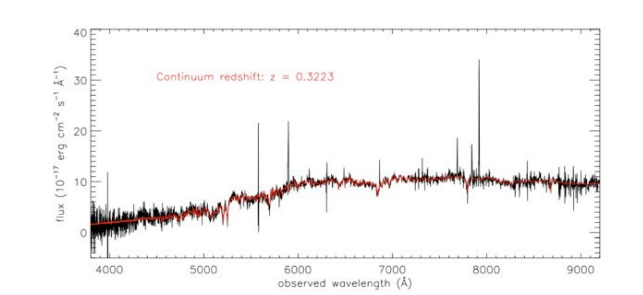
Two main observational startegies for lens detection:

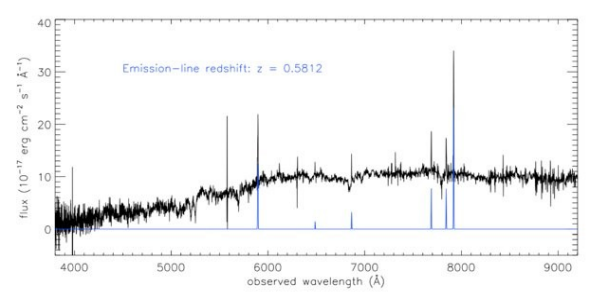
- looking for the presence of emission lines at redshifts higher than that of the target galaxy
- + HST ACS follow-up imaging

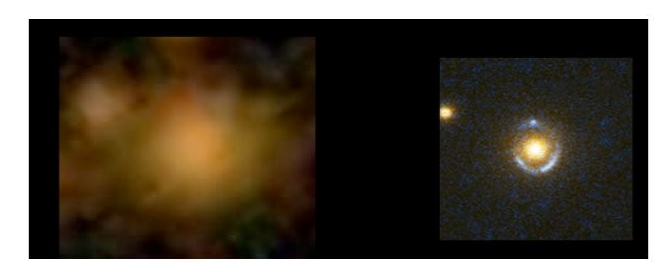


lens candidates selected from SDSS/BOSS data

Sloan Lens ASC Survey **SLACS**BOSS emission-line lens survey **BELLS**







http://www.physics.utah.edu/~bolton/slacs/What_is_SLACS.html

early-type galaxies more likely serve as intervening galaxies

homogeneous sample!

targets: massive red galaxies

 fully automated software (*RingFinder*) looking for tangentially elongated blue features around lensing galaxy

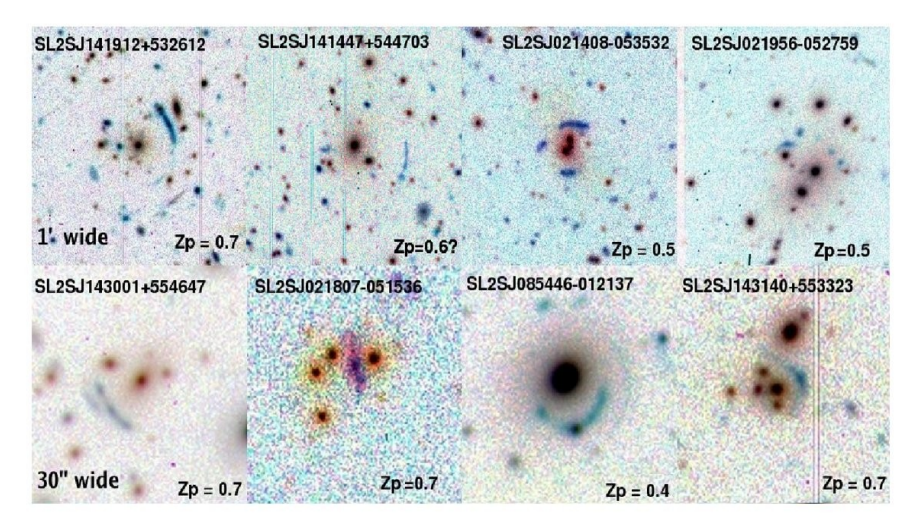
[Gavazzi et al. 2014]



Strong Lensing Legacy Survey **SL2S**

Canada France Hawaii Telescope Legacy Survey (CFHTLS)

they contain most of the stellar mass of the Universe which affects gravitational lensing statistics



Gravitational lenses as a tool for cosmology

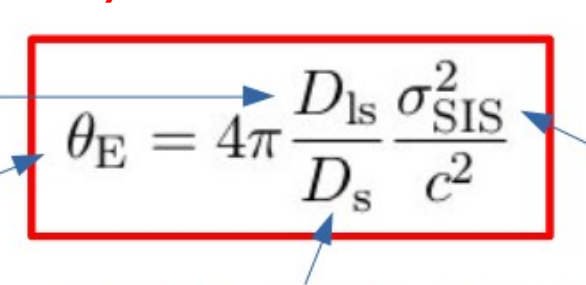
The idea: image separations in the system depend on angular diameter distances to the lens and to the source, which in turn are determined by background cosmology



lenses as standard(izable) rulers!

distance from the lens to the source

from angular image separations (astrometry)



distance from observer to the source



NGC 1316

Singular Isothermal Sphere (SIS)

- the simplest realistic model

$$\rho(r) = \frac{\sigma_v^2}{2\pi G} \frac{1}{r}$$

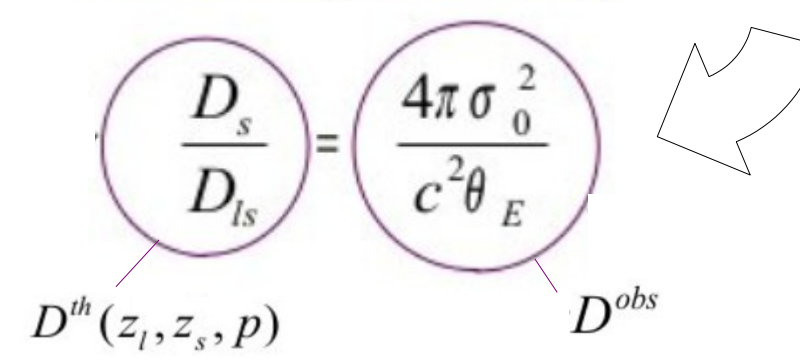
majority of cases the lens is a late-type E/SO galaxy

Koopmans et al. 2006, 2009

velosity dispersion in lensing galaxy (spectroscopy)



Image Credit: D'arcy Kenworthy



'Hubble Tension'

Faster

HKP

TOTAL PROPERTY OF THE PROPERTY

 $\sigma_{\rm SIS}$ lens velocity dispersion is well approximated by σ $_{\rm o}$ - central stellar velocity dispersion (see eg. Grillo et al. 2008)

possibility to constraining the cosmological model provided that we have good knowledge of the lens model

$$D_A(z; \mathbf{p}) = \frac{c}{H_0} \frac{1}{1+z} \int_0^z \frac{dz'}{h(z'; \mathbf{p})}$$

dimensionless expansion rate dependent on redshift z and cosmological model parameters

gets canceled in the distance ratio $\frac{D_s}{D_{ls}}$

Biesiada (2006)

Biesiada, AP (2008)

Biesiada, AP, Malec (2010)

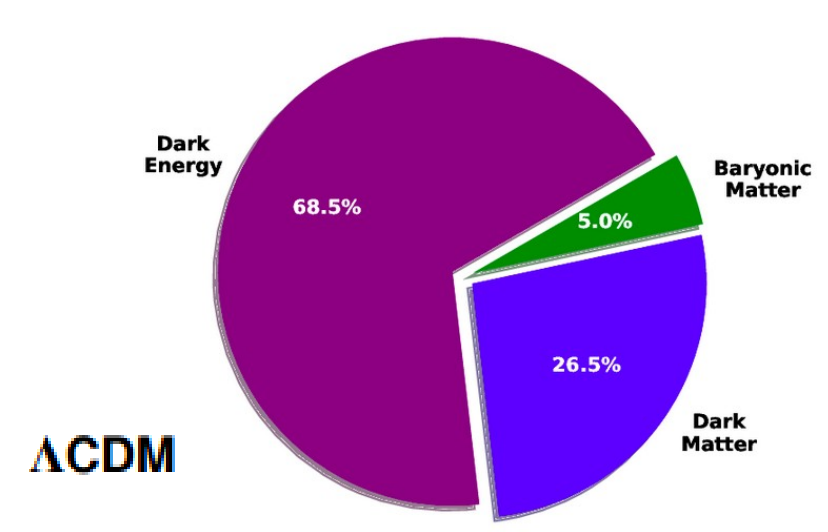
Biesiada, Malec, AP (2011)

method is independent of the Hubble constant's value and is not affected by dust absorption or source evolutionary effects



Cosmological consensus:

most of the energy in the Universe exists in the form of the mysterious dark energy



$$\Omega_{\Lambda} = 0.6889 \pm 0.0056$$
 $\Omega_{M} = 0.3111 \pm 0.0056$

Aghanim et al. (2021)

DE pressure and density (spatially-averaged)

Dark Energy equation of state parameter :



If Dark Energy is a generic dynamical fluid, its equation of state parameter should in general be a function of time.

Time-varying EoS as a Taylor expansion over a(t) (linear order): $w(z) = w_0 + w_a \frac{z}{1+z}$

$$w(z) = w_0 + w_a \frac{z}{1+z}$$

Nobel Prize in Physics 2011





Saul Perlmutter



Brian P. Schmidt



Adam G. Riess

"for the discovery of the accelerating expansion of the Universe through observations of distant supernovae"

Parameter	Planck+SNe+BAO	Planck+BAO/RSD+WL
w ₀	-0.957 ± 0.080	-0.76 ± 0.20
w_a	$-0.29^{+0.32}_{-0.26}$	$-0.72^{+0.62}_{-0.54}$
H_0 [km s ⁻¹ Mpc ⁻¹]	68.31 ± 0.82	66.3 ± 1.8
$\sigma_8 \dots \dots$	0.820 ± 0.011	$0.800^{+0.015}_{-0.017}$
S ₈	0.829 ± 0.011	0.832 ± 0.013
$\Delta \chi^2 \dots$	-1.4	-1.4

Planck 2018 results. Aghanim et al. (2021)

$$w = 0$$
 \longrightarrow dust $w = 1/3$ \longrightarrow radiation $w = -1$ \longrightarrow cosmological constant

CPL parametrization

Chevalier, Polarski (2001); Linder (2003)

$$h^2(z; \mathbf{p}) = \Omega_m (1+z)^3 + (1-\Omega_m)(1+z)^{3(1+w)}$$
 for $XCDM$ cosmology \longrightarrow $\mathbf{p} = \{\Omega_m, w\}$

$$h^2(z; \mathbf{p}) = \Omega_m (1+z)^3 + (1-\Omega_m)(1+z)^{3(1+w_0+w_1)} \exp\left(-\frac{3w_1z}{1+z}\right)$$
 for CPL parametrization $\implies \mathbf{p} = \{\Omega_m, w_0, w_1\}$

lenses as standard(izable) rulers - next steps forward

compilation of 118 lenses from SLD, SLACS, BELLS and SL2S catalogues

$$\rho \sim r^{-\gamma}$$

generalization of the SIS model to spherically symmetric power-law mass distribution

mass inside the Einstein radius:

 $M_{lens} = \frac{c^2}{4G} \frac{D_s D_l}{D_{ls}} \theta_E^2$

[Schneider et al.1992]

$$M_{lens} = M_{dyn}$$

$$\theta_E = 4\pi \frac{\sigma_{ap}^2}{c^2} \frac{D_{ls}}{D_s} \left(\frac{\theta_E}{\theta_{ap}}\right)^{2-\gamma} f(\gamma)$$

dynamical mass inside the aperture projected to lens plane (from solving the Jeans equation):

$$M_{dyn} = \frac{\pi}{G} \sigma_{ap}^2 R_E \left(\frac{R_E}{R_{ap}}\right)^{2-\gamma} f(\gamma)$$
$$= \frac{\pi}{G} \sigma_{ap}^2 D_l \theta_E \left(\frac{\theta_E}{\theta_{ap}}\right)^{2-\gamma} f(\gamma)$$

$$f(\gamma) = -\frac{1}{\sqrt{\pi}} \frac{(5-2\gamma)(1-\gamma)}{3-\gamma} \frac{\Gamma(\gamma-1)}{\Gamma(\gamma-3/2)}$$

$$\times \left[\frac{\Gamma(\gamma/2-1/2)}{\Gamma(\gamma/2)} \right]^2$$

[Koopmans et al. 2005]

making sample more uniform – velocity dispersion correction

new observable:

$$\mathcal{D}^{obs} = \frac{c^2 \theta_E}{4\pi \sigma_{ap}^2} \left(\frac{\theta_{ap}}{\theta_E}\right)^{2-\gamma} f^{-1}(\gamma)$$

$$\sigma_0 = \sigma_{ap}(\theta_{eff}/(2\theta_{ap}))^{-0.04}$$

[Jorgensen et al.1995]

we need to transform all velocity dispersions measured within an aperture to those, measured within circular aperture of radius *Reff / 2*

uncertainties of the effective radius contribute less than 1% to the uncertainty of σ_0

this operation makes our observable more homogeneous for the sample of lenses located at different redshifts

taking into account possible evolution of the power-law index γ with redshift

[Ruff et al. 2011] [Brownstein et al. 2012] [Sonnenfeld et al. 2013]

$$\gamma(z_l) = \gamma_0 + \gamma_1 z_l$$

S. Cao, M. Biesiada, R. Gavazzi, AP & Z.-H. Zhu (2015)

Monte Carlo (CosmoMC package) simulations of the posterior likelihood

$$\mathcal{L} \sim \exp\left(-\chi^2/2\right)$$

$$\chi^2 = \sum_{i=1}^{118} \left(\frac{\mathcal{D}^{th}(z_{l,i}, z_{s,i}; \mathbf{p}, \gamma) - \mathcal{D}^{obs}(\sigma_{0,i}, \theta_{E,i})}{\Delta \mathcal{D}^{obs}_i}\right)^2$$
 5% SLACS Team
$$\delta \mathcal{D} = \frac{\Delta \mathcal{D}}{\mathcal{D}} = \sqrt{4(\delta \sigma_{ap})^2 + (1-\gamma)^2(\delta \theta_E)^2}$$

Table 2 Dark energy (XCDM model and CPL parametrization) constraints obtained on the full 118 strong lensing (SL) sample.

Cosmology (Sample)	w_0	w_1	γ_0	γ_1
XCDM1 (SL; σ_{ap})	$w_0 = -1.45^{+0.54}_{-0.95}$	$w_1 = 0$	$\gamma_0 = 2.03 \pm 0.06$	$\gamma_1 = 0$
XCDM1 (SL; σ_0)	$w_0 = -1.15^{+0.56}_{-1.20}$	$w_1 = 0$	$\gamma_0 = 2.07 \pm 0.07$	$\gamma_1 = 0$
XCDM2 (SL; σ_{ap})	$w_0 = -1.48^{+0.54}_{-0.94}$	$w_1 = 0$	$\gamma_0 = 2.06 \pm 0.09$	$\gamma_1 = -0.09 \pm 0.16$
XCDM2 (SL; σ_0)	$w_0 = -1.35^{+0.67}_{-1.50}$	$w_1 = 0$	$\gamma_0 = 2.13^{+0.07}_{-0.12}$	$\gamma_1 = -0.09 \pm 0.17$
CPL1 (SL; σ_{ap})	$w_0 = -0.15^{+1.27}_{-1.60}$	$w_1 = -6.95^{+7.25}_{-3.05}$	$\gamma_0 = 2.08 \pm 0.09$	$\gamma_1 = -0.09 \pm 0.17$
CPL1 (SL; σ_0)	$w_0 = -1.00^{+1.54}_{-1.05}$	$w_1 = -1.85^{+4.85}_{6.75}$	$\gamma_0 = 2.14^{+0.07}_{-0.10}$	$\gamma_1 = -0.10 \pm 0.18$
CPL2 (SL; σ_{ap})	$w_0 = -0.16^{+1.21}_{-1.48}$	$w_1 = -6.25^{+6.25}_{-3.75}$	$\gamma_0 = 2.08$	$\gamma_1 = -0.09$
CPL2 (SL; σ_0)	$w_0 = -1.05^{+1.43}_{-1.77}$	$w_1 = -1.65^{+4.25}_{-6.35}$	$\gamma_0 = 2.14$	$\gamma_1 = -0.10$
CPL2 (SN)	$w_0 = -1.00 \pm 0.40$	$w_1 = -0.12_{-2.78}^{+1.58}$		

^aIn our fits we separately considered observed velocity dispersions σ_{ap} and corrected velocity dispersions σ_0 , XCDM1 corresponds to assumption of non-evolving power-law index γ , while XCDM2 assumes its evolution $\gamma(z) = \gamma_0 + \gamma_1 z_l$. Fixed prior of $\Omega_m = 0.315$ was assumed according to the Planck data. While fitting CPL parameters we assumed evolving lens mass density with γ_0 and γ_1 as free parameters (CPL1) and then fixed them at best-fit values (CPL2). For comparison fits of CPL parameters using Union2.1 supernovae data (SN) is shown.

lenses as standard(izable) rulers - next move and future prospects

compilation of lenses carefully chosen from known catalogues:

The Lenses Structure and Dynamics (LSD)

Sloan Lens ACS Survey (SLACS)

and its extension – "SLACS for the Masses" (S4TM)

BOSS Emission-Line Lens Survey (BELLS)

BOSS for the GALaxy-Lyα EmitteR sYstems (BELLS GALLERY)

Strong Lensing Legacy Survey (SL2S)

a careful statistical analysis of the data in terms of observables to ensure the robustness of our sample



currently **the largest sample** with both high resolution imaging and stellar dynamical data



previously:

161 galaxy-scale strong lensing systems
Chen, et al. (2019)

To date, **several hundred galaxy-galaxy strong lenses have been discovered** in heterogeneous searches of photometric and spectroscopic survey data

Known lenses are rare because even the most massive galaxies are only capable of deflecting light by an arcsecond or two and only a small fraction of the sky has been observed to sufficient depth and with good enough image resoution to identify a typical Einstein ring.

- □ The 4MOST Strong Lensing Spectroscopic Legacy Survey (4SLSLS)
 - will provide pairs of redshifts for 10 000 strong-lensing galaxies (lenses) and background galaxies (sources)
 - velocity dispersions will also be measured for 5000 lenses

strong lens candidates from:

The Euclid mission



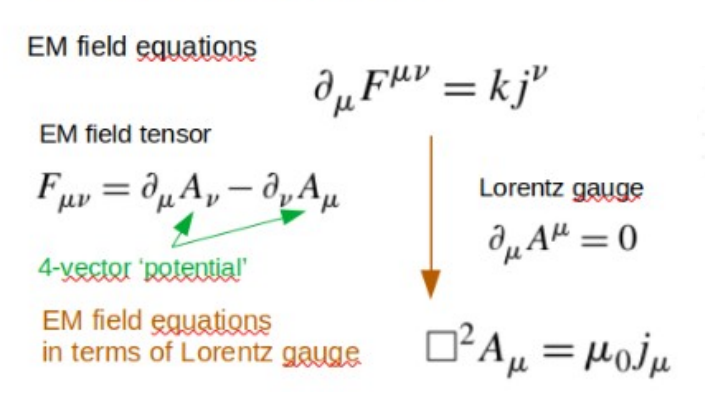
Legacy Survey of Space and Time (LSST)

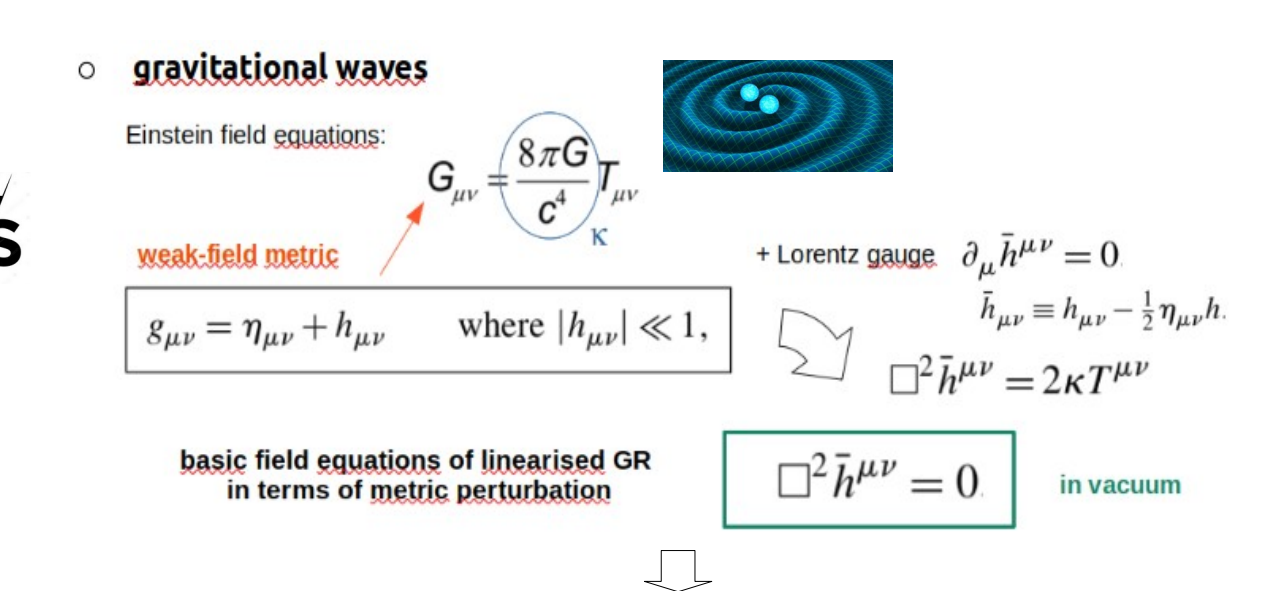
VERA C. RU

about 20 terabytes of data every night during the ten-year survey!

gravitational lenses as a tool for quantum gravity







side effect of similarity between EM and GW:

GW experience the same geometric-optics effects as EM waves!

cosmological redshift gravitational redshift

gravitational lensing

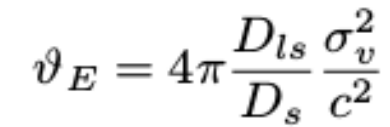
in general relativity the graviton is predicted to be massless!

long range



The idea: In massive graviton scenario Einstein radius is slightly different when compared to the standard case

in SIS model + standard physics:





in SIS model + massive graviton:

$$\vartheta_{E,GW} = \vartheta_E (1 + \frac{m_{GW}^2 c^4}{2E^2})$$

Lowenthal, PRD (1973)



small extra term

GR naturally lose it's applicability at curvature singularities i.e. the Planck length

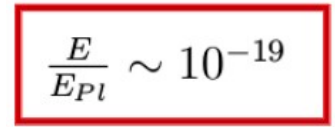
$$l_{Pl} = \sqrt{\hbar G/c^3} \sim 10^{-33} \text{cm}$$

or equivalently – Planck energy:

$$E_{PL} = \sqrt{\hbar c^3/G} \sim 10^{19} \text{GeV}$$

sensitivity requirements for tests are very strict

- we need accuracy better than

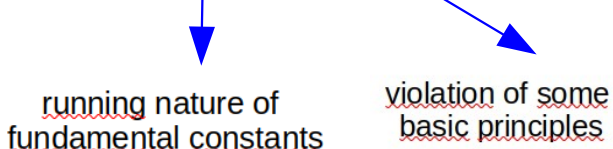


no experimental indication which way is correct?



effective phenomenology e.g.









Fierz & Pauli (1930)



Wolfgang Pauli



Markus Eduard Fierz

first theory of a massive spin-2 field propagating on a flat spacetime

Fierz-Pauli mass term,

$$\mathcal{L}_{ ext{FP}} = m^2 \left(h^{\mu
u} h_{\mu
u} - \left(\eta^{\mu
u} h_{\mu
u}
ight)^2
ight)$$

do not uniformly reduce to those of general relativity in the limit m o 0



vDVZ discontinuity.

at small scales when one takes into account nonlinear effects!

(shorter tan the Compton wavelength of the graviton)



de Rham-Gabadadze-Tolley (dRTG) gravity (2010)

Ghost-free massive gravity



Andrew Tolley



Claudia de Rham





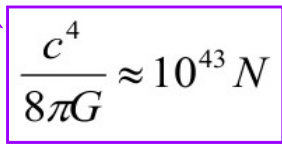
Gregory Gabadadze

Searching for QG - lesson from GW detection history

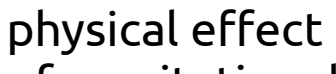
do GWs really exist and, if yes, can we detect them directly?

$$G_{\mu\nu} = \frac{8\pi G}{c^4} T_{\mu\nu} \qquad \qquad T_{\mu\nu} = \frac{c^4}{8\pi G} G_{\mu\nu}$$
 strain tensor

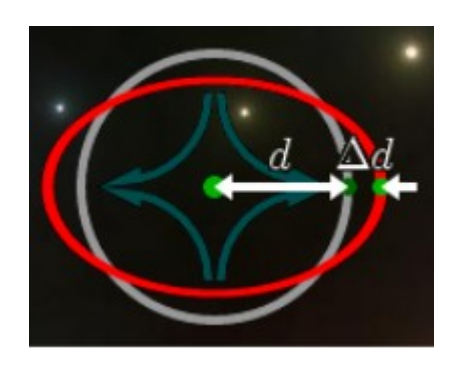
(analogy to the Hooke's Law)



elastisity modulus



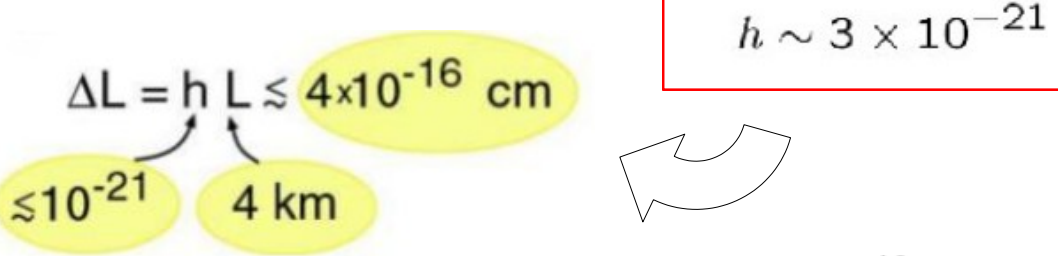
of gravitational wave: $h = \Delta L/L$



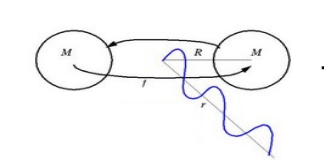
wave intensity: relative amplitude of deformation!

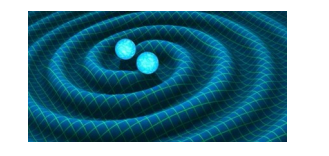
$$h = \frac{2\Delta d}{d}$$

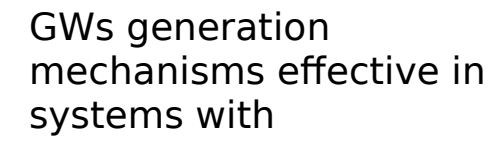
For
$$1M_{\odot} \Rightarrow R_s = 2GM_{\odot}/c^2 = 3$$
 km If $v \approx c$, then at $r = 15$ Mpc:



the proton radius is $\sim 10^{-13}$ cm ...







- sizes of the order of Schwarzchild radius
- velocities of the order of speed of light in vacuum

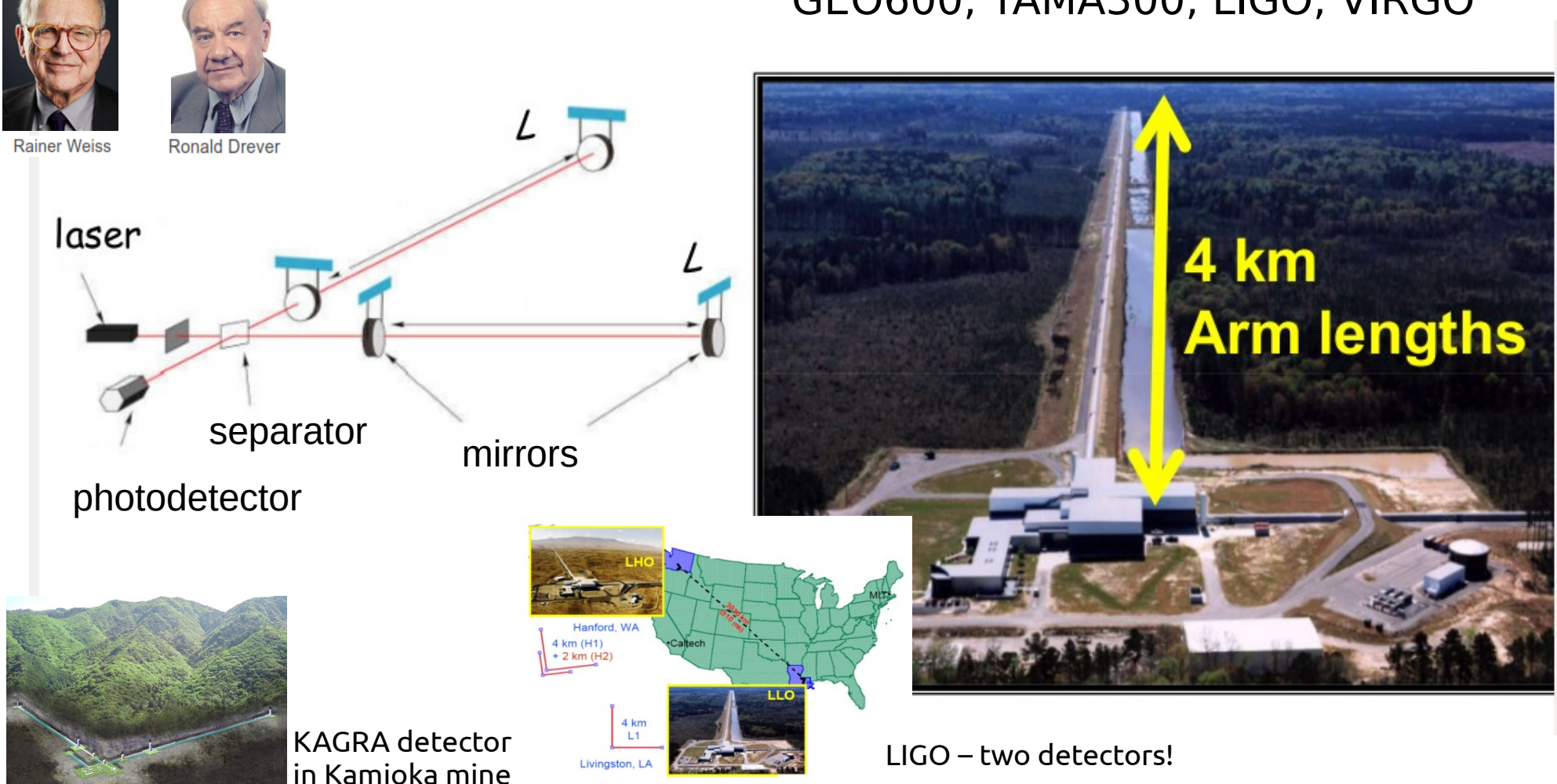


compact object binaries: BH-BH, BH-NS, NS-NS

Interferometric detectors:



GEO600, TAMA300, LIGO, VIRGO



PSR B1913+16

GW signal doscovered 100 years after formulation of GR

apart from Hulse and Tylor indirect proof (Nobel Prize 1993)















ALFR. NOBEL

Kip Barry C. **Thorne** Barish

C. Reiner **Meiss**

Observation of Gravitational Waves from a Binary Black Hole Merger

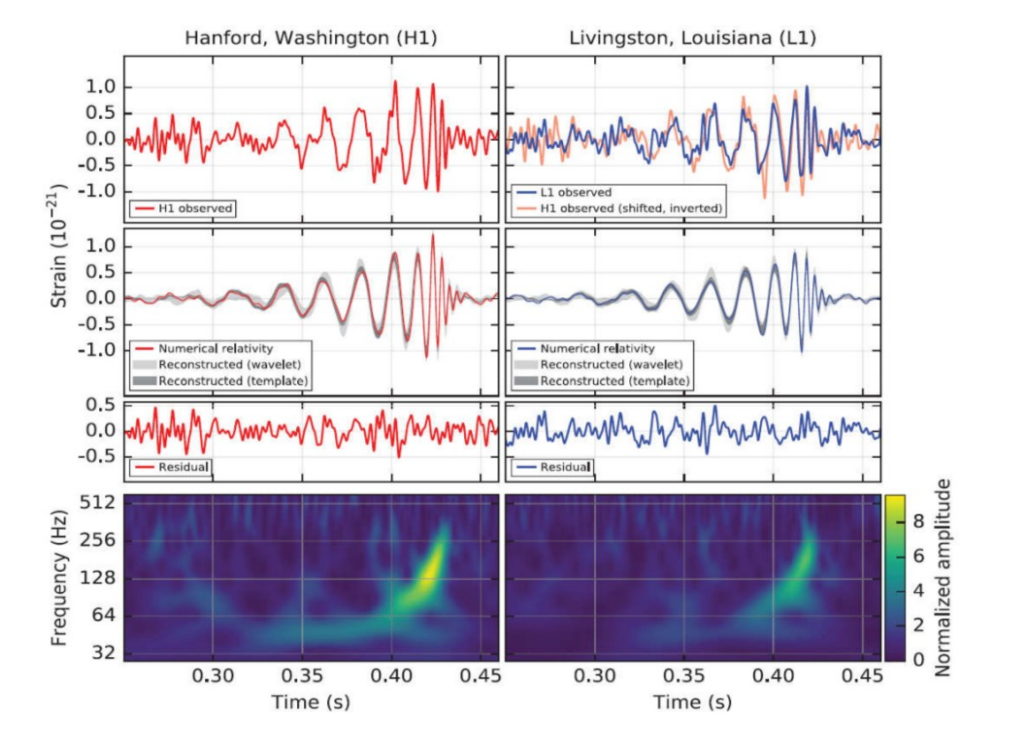
B. P. Abbott *et al.**

(LIGO Scientific Collaboration and Virgo Collaboration)

(Received 21 January 2016; published 11 February 2016)

On September 14, 2015 at 09:50:45 UTC the two detectors of the Laser Interferometer Gravitational-Wave Observatory simultaneously observed a transient gravitational-wave signal. The signal sweeps upwards in frequency from 35 to 250 Hz with a peak gravitational-wave strain of 1.0×10^{-21} . It matches the waveform predicted by general relativity for the inspiral and merger of a pair of black holes and the ringdown of the resulting single black hole. The signal was observed with a matched-filter signal-to-noise ratio of 24 and a false alarm rate estimated to be less than 1 event per 203 000 years, equivalent to a significance greater than 5.1σ . The source lies at a luminosity distance of 410^{+160}_{-180} Mpc corresponding to a redshift $z=0.09^{+0.03}_{-0.04}$. In the source frame, the initial black hole masses are $36^{+3}_{-4}M_{\odot}$ and $29^{+4}_{-4}M_{\odot}$, and the final black hole mass is $62^{+4}_{-4}M_{\odot}$, with $3.0^{+0.5}_{-0.5}M_{\odot}c^2$ radiated in gravitational waves. All uncertainties define 90% credible intervals. These observations demonstrate the existence of binary stellar-mass black hole systems. This is the first direct detection of gravitational waves and the first observation of a binary black hole merger.

DOI: 10.1103/PhysRevLett.116.061102



2017 Nobel Prize in Physics

"For decisive contributions to the LIGO detector and the observation of gravitational waves."

GW150914

- · first evidence for the existence of BBH
- first evidence for relativistic evolution up to the merger stage of BBH systems
- validation of gravitational radiation formulas

Estimated source parameters

90% credible interval.

Quantity	Value	Upper/Lower error estimate	Unit
Primary black hole mass	36.2	+5.2 -3.8	M sun
Secondary black hole mass	29.1	+3.7 -4.4	M sun
Final black hole mass	62.3	+3.7 -3.1	M sun
Final black hole spin	0.68	+0.05 -0.06	
Luminosity distance	420	+150 -180	Мрс
Source redshift, z	0.09	+0.03 -0.04	
Energy radiated	3.0	+0.5 -0.5	M sun

PHYSICAL REVIEW LETTERS

Hiahliahts

Recent

Accepted

Collection

Authors

Referee

Searc

Pr

Abo

Speed of Gravitational Waves from Strongly Lensed Gravitational Waves and Electromagnetic Signals

Xi-Long Fan, Kai Liao, Marek Biesiada, Aleksandra Piórkowska-Kurpas, and Zong-Hong Zhu Phys. Rev. Lett. **118**, 091102 – Published 2 March 2017

$$\vartheta_E \neq \vartheta_{E,GW}$$
 \Box

$$\Delta t_{GW} \neq \Delta t_{\gamma}$$

$$\Delta t_{SIS} = \frac{32\pi^2}{H_0} \left(\frac{\sigma}{c}\right)^4 y \frac{\widetilde{r}(z_l)\widetilde{r}(z_l, z_s)}{\widetilde{r}(z_s)}$$

source-lens misalignment $y=eta/\vartheta_E$

difference between time delays measured independently in GW and EM windows

$$\Delta t_{\gamma} - \Delta t_{GW}$$

- method based on modified dispersion relation and thus independent of a particular non-standard model of gravity
- method is differential in nature and thus free from any assumptions regarding intrinsic timelag between EM and GW signal emission

general form for bound on v_{GW} valid for a broad set lens models

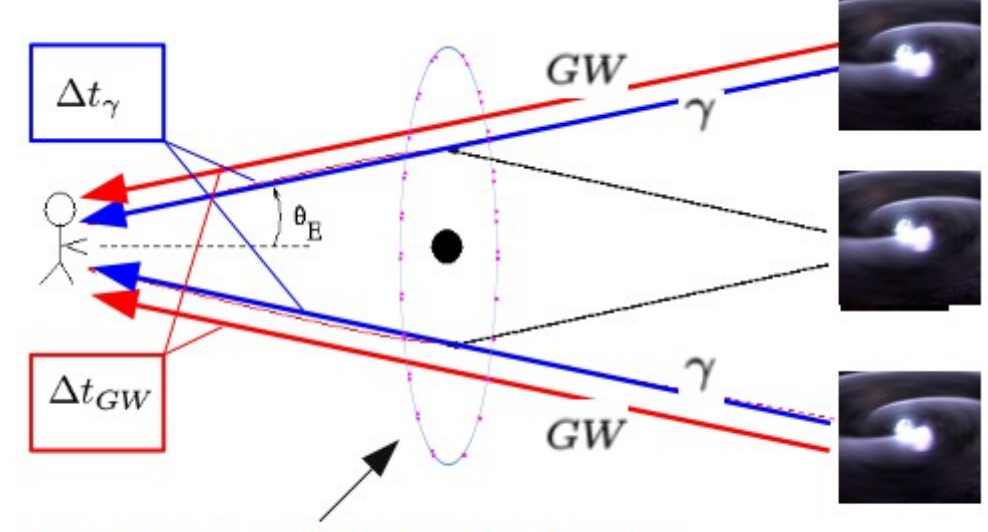
 $1-\left(rac{v_{GW}}{c}
ight)^2 \leq rac{\delta T}{\Delta t_{\gamma} F_{
m lens}(z_l,z_s)}$

factor related to lens model and cosmology $F_{\rm lens}(z_l,z_s) \sim O(1)$

we can constrain **directly** speed of GWs with lensing



timing



time delay is produced at lens location

results doesn't depend strongly on cosmology

lenses as a tool for quantum gravity - future prospects











A2 A bird's eye view image of KAGRA. The 3-km arms and the center part are illustrated.

from 12 September 2015 to 19 January 2016,

from 30 November 2016 to 25 August 2017,

from 1 April to 30 September 2019

from 1 November 2019 O₃b suspended in March 2020

O4 currently planned to end on 7 October 2025 at 15:00 UTC

Hundreds of GW signals registered so far!

GW17081

NS-NS merger

GW190814

B.P.Abbott et al. [LSC, Virgo Collab.], Phys. Rev. X 13(4):041039 (2023) R.Abbott et al. [LSC, Virgo Collab.], arXiv:2010.14527 [gr-qc] (2020) R.Abbott et al. [LSC, Virgo Collab.], arXiv:2010.14533 [astro-ph] (2020) B.P.Abbott et al. [LSC, Virgo Collab.], Phys. Rev. X 9, 031040 (2019)

Next generation GW detectors:



Fig. 1. Orbit of DECIGO. Four clusters of

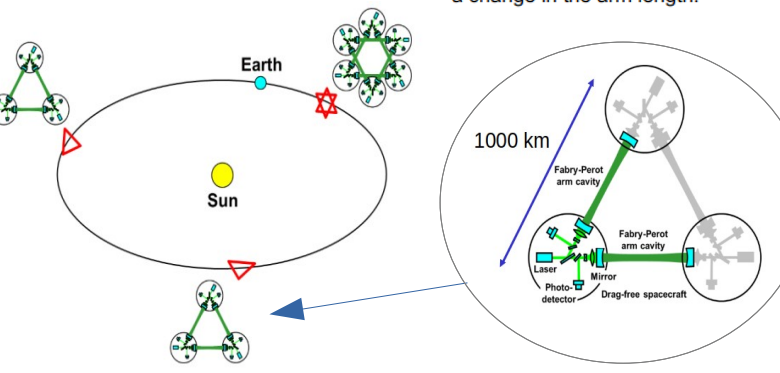
at the same position and the other two at

different positions.

DECIGO are put in the heliocentric orbit: two

https://decigo.jp/index E.html

Fig. 2. Conceptual design of DECIGO. One cluster of DECIGO consists of three drag-free spacecraft. FP cavities are used to measure a change in the arm length.

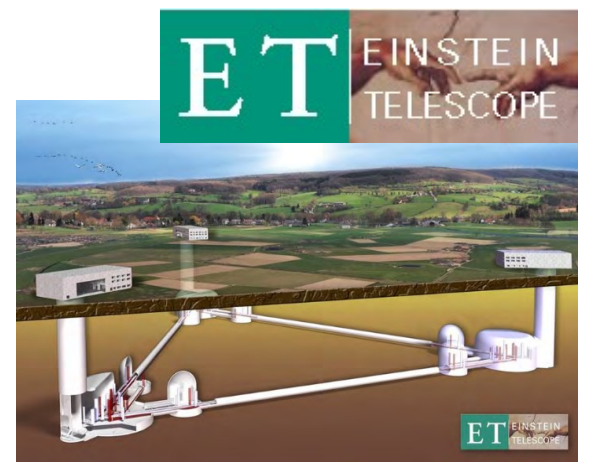


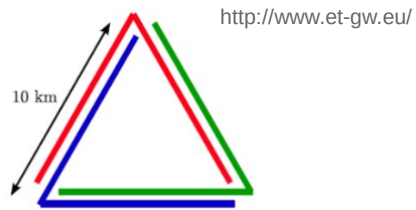
Nakamura T., et al. (2016) Kawamura, S., et al. (2019)





Figure 2: Artist's rendition of the LISA mission (image credit: ESA)





Goldstein, A., et al., ApJL 2017, 848, L14. Yagi, K. & Seto, N. 2011, PRD, 83, 044011

single triangular detector unit is equivalent for two standard L-shaped interferometers rotated by 45°



f: 0.1 mHz - 100 mHz



f: 1 mHz – 100 Hz

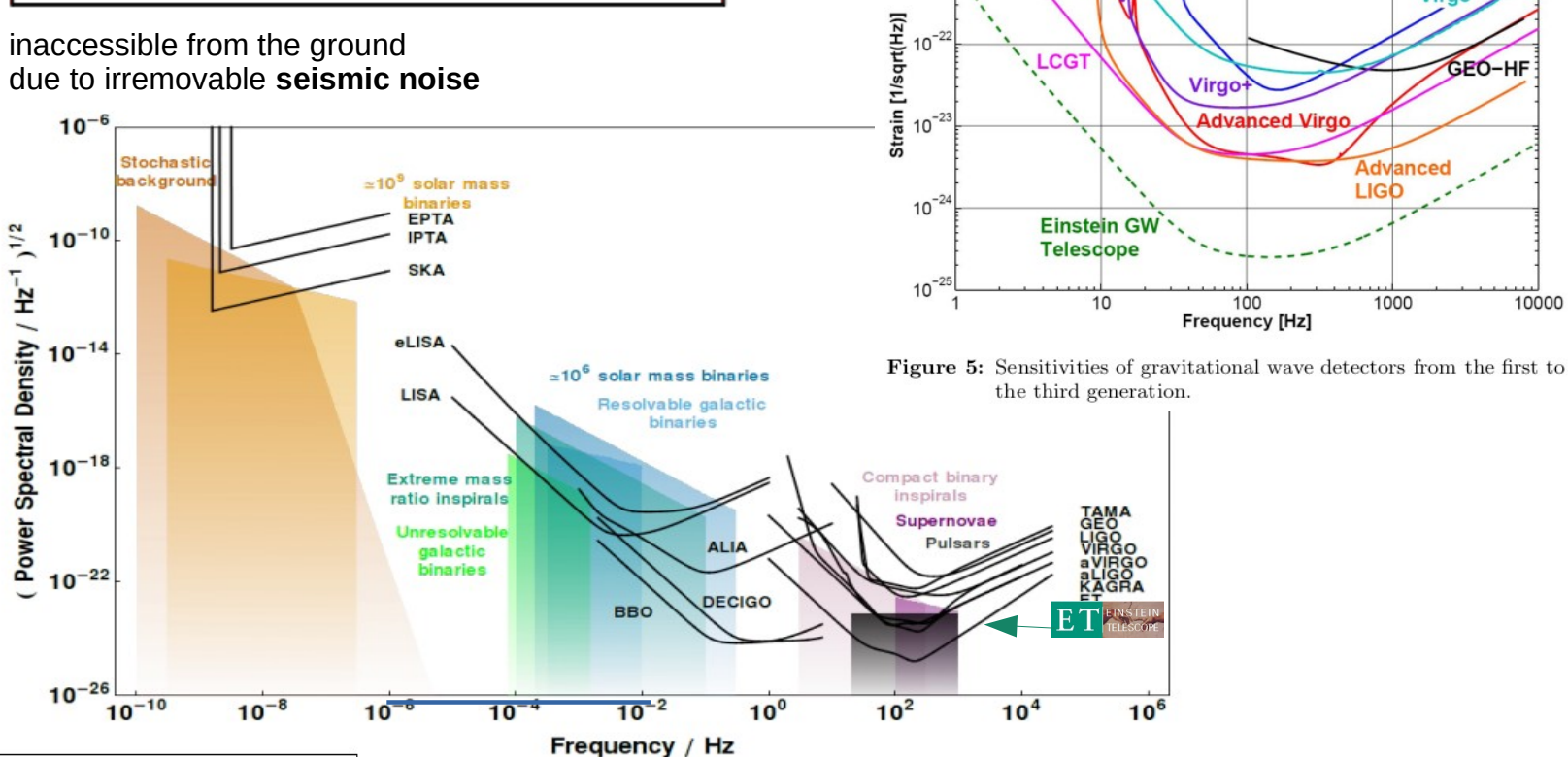


multifrequency

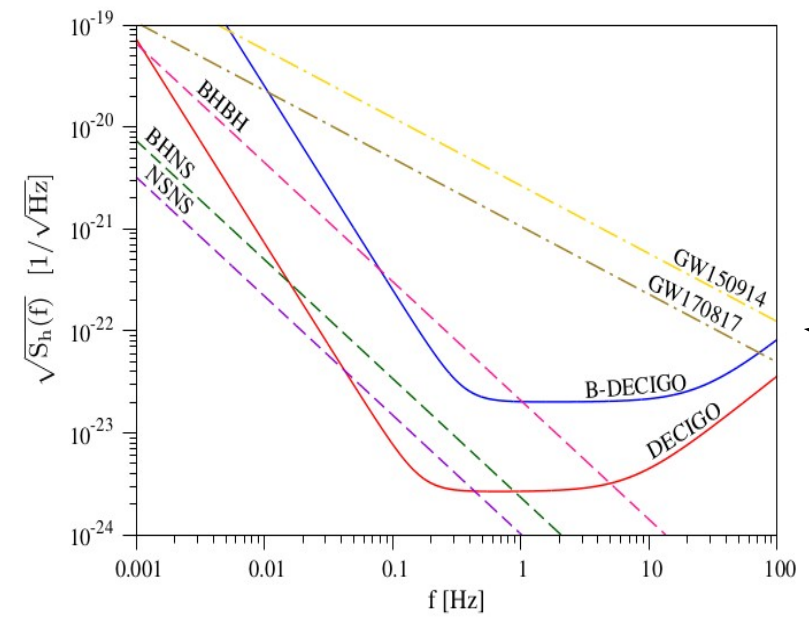
GW astrophysics!

broadening the GW spectrum to lower frequencies (lower than 1 Hz)

inaccessible from the ground



Remark:



DECIGO sensitivity significantly affected by unresolved BH-BH systems; B-DECIGO affected much less

10⁻²¹

 $t_c = 1.03 \times 10^6 \text{ s} (\mathcal{M}_z/30.1 \ M_{\odot})^{-5/3} (f/0.1 \ \text{Hz})^{-8/3}$

GW150914 and GW170817 could have been visible in (B-)DECIGO band for ~ 10 days and ~ 7 yrs prior to coalescence with large numbers of GW cycles



Isoyama, S. et al., Prog. Theor. Exp. Phys. 073E01 (2018)

Auriga

LIGO

1000

Virgo

GEO-HF

10000

LIGO

Advanced Virgo

100

Frequency [Hz]

A. Piórkowska-Kurpas et al, ApJ 908 196 (2021)

lenses as a tool for quantum gravity - perspectives:

for galaxy-galaxy strong lensing with $z_l = 1$ and $z_s = 2$





$$\Delta t_{\gamma,GW} = \frac{1}{2H_0} (1+z_s)^2 I_2(0,z_s)$$
 \Box $1 - \left(\frac{v_{GW}}{c}\right)^2 \le 9.92 \times 10^{-22}$

$$1 - \left(\frac{v_{GW}}{c}\right)^2 \le 9.92 \times 10^{-22}$$

EM counterpart of NS-NS or NS-BH mergers visible as:

- kilonovae duration of order of days
- short GRBs duration of order of 0.1 1s
- duration of order of ms

P.S.Cowperthwaite and E.Berger, ApJ 814, 25 (2015)

D.B. Fox et al., Nature 437, 845 (2005)

D. J. Champion et al., MNRAS 10.1093 (2016) D.Thornton et al., Science 341, 53 (2013)

lensed NS-NS mergers!





jet collimation



~10% of NS-NS systems will be aligned as to give observable SGRBs

Let's do some statistics...

Detection rates for aLIGO and ET

Source	BNS	NS-BH	BBH
Rate $(Mpc^{-1} Myr^{-1})$	0.1-6	0.01 – 0.3	$2 \times 10^{-3} - 0.04$
Event Rate (yr^{-1}) in aLIGO	0.4 - 400	0.2 – 300	2 - 4000
Event Rate (yr^{-1}) in ET	$\mathcal{O}(10^3 - 10^7)$	$\mathcal{O}(10^3 - 10^7)$	$\mathcal{O}(10^4 - 10^8)$

M. Biesiada et al. JCAP10(2014)080

Yearly detection rate for DECIGO

Evolutionary scenario	standard	optimistic CE	delayed SN	high BH kicks
NS-NS				
low-end metallicity	233.1	119.	335.5	3054.4
high-end metallicity	439.6	203.9	707.3	8807.7
BH-NS				
low-end metallicity	2688.9	1239.5	1838.6	1877.6
high-end metallicity	2000.	1314.6	1614.5	1613.7
BH-BH				
low-end metallicity	207755.2	384698.	178991.7	20125.8
high-end metallicity	166436.	360001.5	145583.5	15379.5
TOTAL				
low-end metallicity	210677.2	386056.5	181165.8	25057.8
high-end metallicity	168875.6	361520	147905.3	25800.9









Big catalogs of inspiral events up to cosmological distances



Some of them would be gravitationally lensed

First Multimessenger Transient

GW170814

GWs LIGO/VIRGO



GRB 170817A

γ-rays Fermi/GBM

11 hours after the merger

SSS17a / **AT 2017qfo**

bright optical transient

in NGC 4993

multi-wavelength evolution within the first 12-24 hr

Follow-up observations:

UV-blue transient ~15h after merger X-ray emission ~9 days after merger

IPN Fermi /

INTEGRAL

~16 days after merger radio emission

[Multi-messenger Observations of a Binary Neutron Star Merger; ApJL, 848:L12, 2017]



lensed NS-NS mergers

GW lensing in ET discussed in papers:



DLT40 -20.5 d



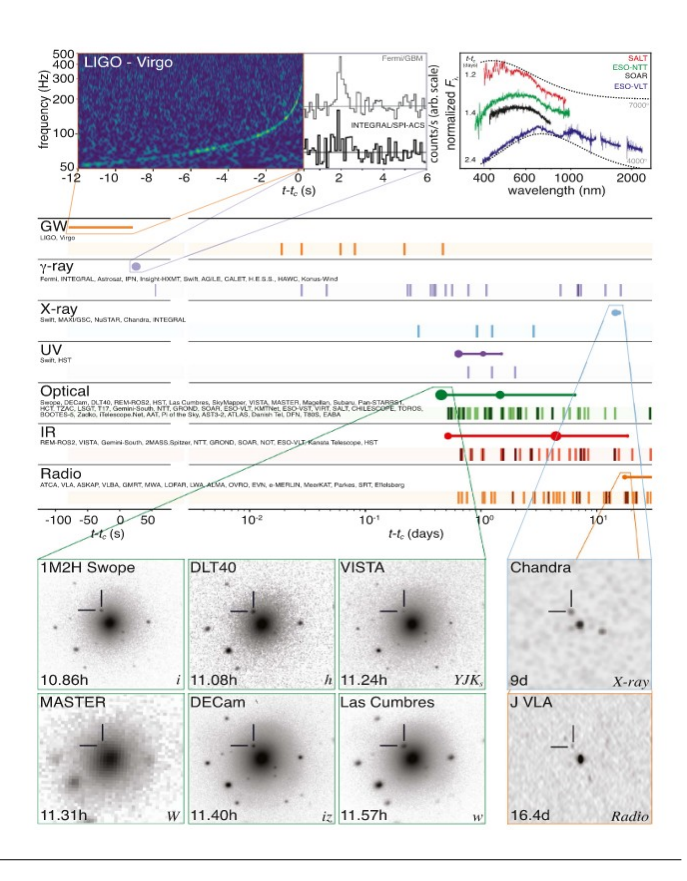
- A. Piórkowska et al. **JCAP10(2013)022** (NS-NS only)
- M. Biesiada et al. **ICAP10(2014)080** (full DCO: NS-NS, BH-NS, BH-BH)
- X. Ding et al. JCAP12(2015)006 (relaxing intrinsic SNR=8 demand; magnification bias)

robust prediction:

50-100 lensed DCO events per year

BH-BH systems contribute 91 – 95%; NS-NS systems 1 – 4%

~a few lensed NS-NS /yr



Einstein Telescope

- Increased sensitivity great expectations
- Big catalogs of inspiral events up to cosmological distances
- Multi-messenger astrophysics
- Some of them would be gravitationally lensed

results corrected for Earth's rotation effect:

L. Yang et al. ApJ 874, 139 (2019)



SNR above threshold of 8

Yagi & Seto 2011 Isoyama et al. 2018

Inspiraling Double Compact Object Detection and Lensing Rate: Forecast for DECIGO and B-DECIGO

Aleksandra Piórkowska-Kurpas^{1,2}, Shaoqi Hou³, Marek Biesiada^{1,4}, Xuheng Ding^{3,5}, Aleksandra Piórkowska-Kurpas^{1,2}, Shaoqi Hou³, Marek Biesiada^{1,4}, Nuheng Ding^{3,5}

Shuo Cao¹, Xilong Fan³, Seiji Kawamura⁶, and Zong-Hong Zhu^{1,3}

Published 2021 February 24 • © 2021. The American Astronomical Society. All rights reserved.

The Astrophysical Journal, Volume 908, Number 2

Citation Aleksandra Piórkowska-Kurpas et al 2021 ApJ 908 196

50 lensed events per year few lensed events per year

only BH-BH systems



confusion noise of unresolved systems influence our ability to detect inspiraling DCO systems optical depth corrected for finite duty cycle of detector



merger rates according to Dominik et al. 2013

https://www.syntheticuniverse.org

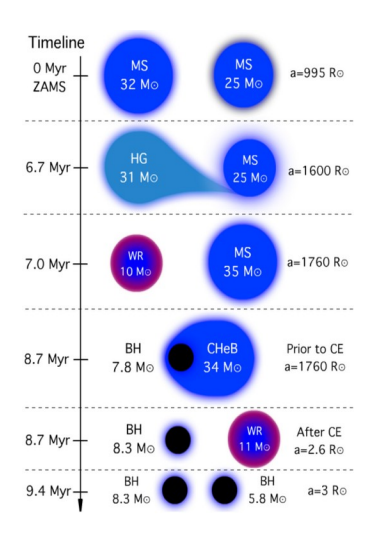
StarTrack code

4 binary evolution scenarios:

2 galaxy metallicity evolution models

"high-end" "low-end"

- 1. Standard
- 2. Optimistic Common Envelope (OCE)
- 3. Delayed SN explosion
- 4. High BH kick



expected numbers of lensed GW events from inspiraling DCOs

		DECIGO	T_s	$urv = 4 \ yrs.$		DECIGO		
Evolutionary scenario	standard	optimistic CE	delayed SN	high BH kicks	standard 4vrs	optimistic CE 4yrs	delayed SN 4vrs	high BH kicks 4vrs
NS-NS low-end metallicity high-end metallicity BH-NS	0. 0.	0. 0.	0. 0.	0.07 0.29	6.1 6.0	53.4 56.7	6.4 6.5	6.1 6.2
low-end metallicity high-end metallicity	$0.2 \\ 0.21$	$0.02 \\ 0.03$	$0.15 \\ 0.2$	0.38 0.39	6.2 5.7	$\frac{9.4}{9.8}$	$\frac{2.9}{2.7}$	$0.7 \\ 0.7$
low-end metallicity high-end metallicity	66.91 65.07	58.12 71.28	$62.86 \\ 61.41$	10.04 8.46	$146.4 \\ 125.6$	$324.0 \\ 312.0$	$125.2 \\ 106.4$	11.4 9.4
		B-DECIGO				B-DECIGO		
Evolutionary scenario	standard	optimistic CE	delayed SN	high BH kicks	standard 4vrs	optimistic CE 4vrs	delayed SN 4yrs	high BH kicks 4vrs
NS-NS low-end metallicity high-end metallicity	0. 0.	0. 0.	0. 0.	0. 0.	0.0001 0.0002	$0.0004 \\ 0.0004$	$0.0001 \\ 0.0002$	$0.0001 \\ 0.0001$
BH-NS low-end metallicity high-end metallicity	$0.2 \\ 0.21$	0.02 0.03	$0.15 \\ 0.2$	0.38 0.39	$0.07 \\ 0.03$	$0.2 \\ 0.1$	$0.04 \\ 0.02$	$0.006 \\ 0.005$
BH-BH low-end metallicity high-end metallicity	9.25 13.66	5.42 10.94	9.2 14.78	2.73 2.25	48.8 38.3	134.1 121.2	$\frac{40.3}{31.3}$	$\frac{3.1}{2.4}$

lensing rates calculated if all accessible sources were resolvable ...

lenses as a tool for quantum gravity - next step:

analysis performed on the sample of 167 strong gravitational lensing systems

Observation: discrepancy between M_{lens} and M_{dyn}

Within the Einstein radius, we suppose that $M_{lens} = M_{dyn}$

 $M_{lens} = \frac{c^2}{4G} \frac{D_s D_l}{D_l} \theta_E^2$ mass inside the Einstein radius:

dynamical mass inside the aperture projected to lens plane

(from solving the Jeans equation):

$$M_{dyn} = \frac{\pi}{G} \sigma_{ap}^2 R_E \left(\frac{R_E}{R_{ap}}\right)^{2-\gamma} f(\gamma)$$
$$= \frac{\pi}{G} \sigma_{ap}^2 D_l \theta_E \left(\frac{\theta_E}{\theta_{ap}}\right)^{2-\gamma} f(\gamma)$$

 $f(\gamma) = -\frac{1}{\sqrt{\pi}} \frac{(5-2\gamma)(1-\gamma)}{3-\gamma} \frac{\Gamma(\gamma-1)}{\Gamma(\gamma-3/2)}$

 $\times \left[\frac{\Gamma(\gamma/2-1/2)}{\Gamma(\gamma/2)}\right]^2$

Idea: $\theta_E^{obs} = \theta_E + \Delta \theta_E$

'pure' Einstein radius

i.e. Einstein radius as is expected within standard theory

some correction which depends on the details of a particular QG model (i.e. on its parameters)

$$\theta_E^{obs} = (1 + \alpha)\theta_E$$

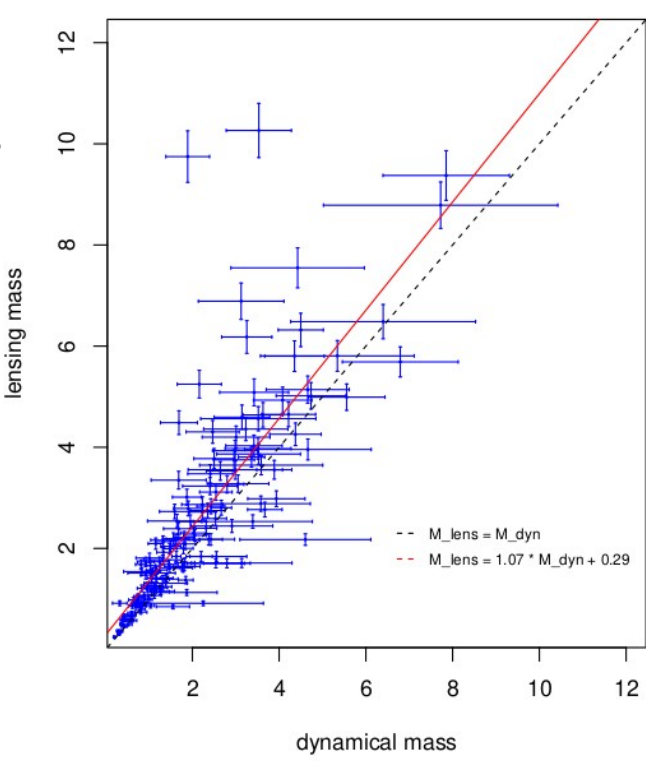
Li et al. ApJ (2018)

e.g. within massive photon scenario:

$$\theta_E^{\gamma} = (1 + \alpha_{\gamma}) \theta_E$$
, where $\alpha_{\gamma} = \frac{m_{\gamma}^2 c^4}{2E^2}$

Lowenthal, PRD (1973)

for SIS model



For the SIS mass model, y = 2 and f(y) = 1,

$$egin{align} M_{
m dyn}(< heta_E) &= rac{\pi}{G} \sigma_{
m ap}^2 D_l heta_E \ &= rac{\pi}{G} \sigma_{
m ap}^2 R_E. \end{split}$$

Li et al. ApJ (2018)

the stringest upper limit for the photon mass is: (from pulsar timing and fast radio bursts FRBs data)

 $m_{\gamma} \leq 9.52 \times 10^{-46} kg$ (which is equivalent to $m_{\gamma} \le 5.34 \times 10^{-10} eVc^{-2}$) $\alpha_{\gamma} \ge 9.3 \times 10^{-10}$ Wang et al. (2024)

$$M_{lens} = M_{dyn}$$

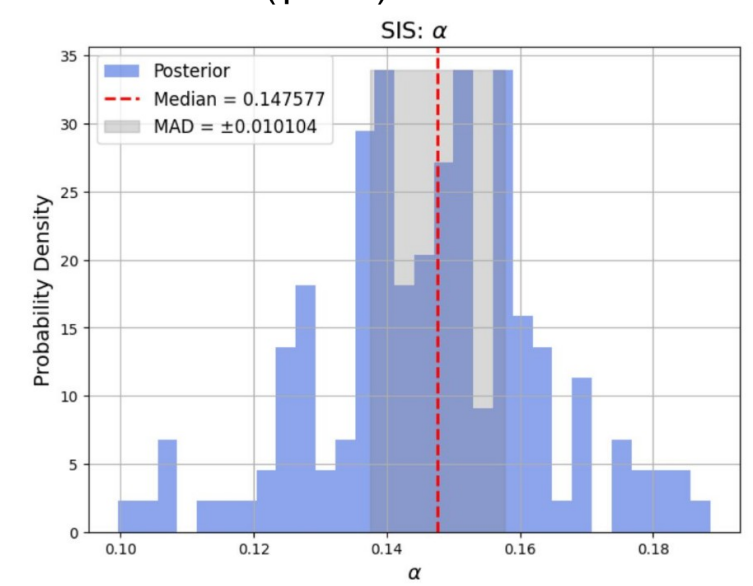
$$\Box$$

$$\frac{c^2}{4G} \frac{D_l D_s}{D_{ls}} \theta_E^2 = \frac{\pi}{G} \sigma_{ap}^2 D_l \theta_E \left(\frac{\theta_E}{\theta_{ap}}\right)^{2-\gamma} f(\gamma)$$

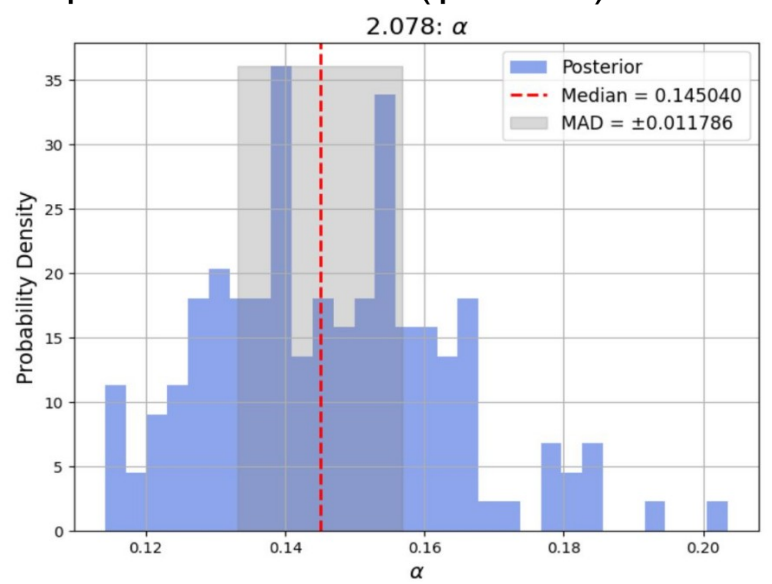
$$(heta_E)^{th} = (1+lpha) igg[4\pi (rac{\sigma_{ap}}{c})^2 rac{D_{ls}}{D_s} (heta_{ap})^{\gamma-2} f(\gamma) igg]^{rac{1}{\gamma-1}}$$
 $\chi^2 = \sum_i rac{igg[(heta_E)_i^{
m obs} - (heta_E)_i^{
m th} igg]^2}{ig(\Delta (heta_E)_i^{
m obs} ig)^2 + ig(\Delta (heta_E)_i^{
m th} igg)^2}$

Preliminary results

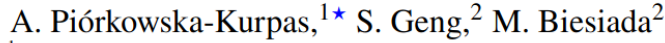
SIS model (y=2.0)



power-law model (y=2.078)



Mass discrepancy between strong lensing and galaxy dynamics observations



¹Institute of Physics, University of Silesia, 75 Pułku Piechoty 1, 41-500 Chorzów, Poland



²National Centre for Nuclear Research, Pasteura 7, 02-093 Warsaw, Poland

